ACS APPLIED MATERIALS & INTERFACES
Research Article
www.acsami.org

Suppression of Degradation Induced by Negative Gate Bias and Illumination Stress in Amorphous InGaZnO Thin-Film Transistors by Applying Negative Drain Bias

Dapeng Wang,*[†] Mai Phi Hung,[†] Jingxin Jiang,[†] Tatsuya Toda,[†] and Mamoru Furuta*[†,‡]

[†]Department of Environmental Science and Engineering, Kochi University of Technology, Kami, Kochi 782-8502, Japan
[‡]Institute for Nanotechnology, Kochi University of Technology, Kami, Kochi 782-8502, Japan

ABSTRACT: The effect of drain bias (V_{DS}) on the negative gate bias and illumination stress (NBIS) stability of amorphous InGaZnO (a-IGZO) thin-film transistors was investigated using a double-sweeping gate voltage (V_{GS}) mode. The variation in the transfer characteristics was explored using current−voltage and capacitance−voltage characteristics. In the initial stage (<1000 s) of NBIS with grounded V_{DS} (V_{GS} = −40 V and V_{DS} = 0 V), the transfer characteristics shifted negatively with an insignificant change in the subthreshold swing (SS) because of hole trapping at an IGZO/gate insulator interface. On the other hand, on-current degradation was observed and was accelerated in the forward measurement as the NBIS duration increased. The results indicated that NBIS induced donor-like defects near the conduction band; however, the transfer curves in the reverse measurement shifted positively without on-current and SS degradations. It was found that the degradations were enhanced by applying a positive V_{DS} bias (V_{GS} = −40 V and V_{DS} = 40 V); in contrast, they could be reduced by applying a small negative V$_{DS}$ of V_{DS} > V_{GS} (V_{GS} = −40 V and V_{DS} = −20 V). Furthermore, it was confirmed that the NBIS degradations could be suppressed by applying a large negative V_{DS} bias of V_{DS} < V_{GS} (V_{GS} = −40 V and V_{DS} = −60 V) during NBIS.

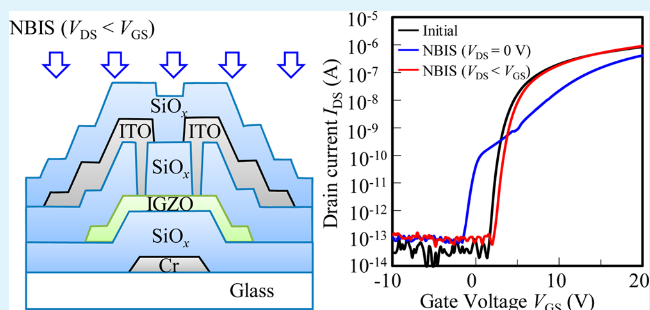

KEYWORDS: *InGaZnO, thin-film transistors, negative gate bias and illumination stress, drain bias, degradation mechanism*

1. INTRODUCTION

In the last decade, transparent amorphous oxide semiconductor-based thin-film transistors (TFTs), using amorphous indium gallium zinc oxide (a-IGZO) as an active layer, have been much investigated for their application in next-generation active-matrix liquid crystal displays (AM-LCDs) and active-matrix organic light-emitting diodes (AM-OLEDs).[1−6] Compared with conventional amorphous silicon TFTs, an a-IGZO TFT exhibits many excellent electrical properties, such as high mobility (μ), low value of subthreshold swing (SS), and good transparency to visible light.[7−11] However, device reliabilities under gate bias, thermal, and light stresses are recognized as issues remaining to be resolved for commercial products. Thus, many researches have been carried out to improve the reliabilities of oxide TFTs under the above-mentioned stress conditions. In particular, degradation under negative gate bias and illumination stress (NBIS) has been recognized as a crucial issue of oxide TFTs. This is because the TFTs in AM-LCDs and AM-OLEDs are frequently negatively biased and exposed to backlight or ambient light during operation.[12−15] Until now, three possible mechanisms have been proposed for NBIS degradation: photogenerated hole trapping in the gate insulator (GI) or at the GI/semiconductor interface,[16−21] defect creation in the active layer,[22−24] and donor-like defect creation combined with a buildup of positive charge at the GI/active layer interface.[25] The stability of oxide TFTs under long-term current operation is also an important issue for pixel signal level and emission intensity in current-driven AM-OLEDs.[26,27] However, the degradation of amorphous oxide TFTs under a combination of NBIS and drain bias (V_{DS}) has been rarely reported.

In this study, the variation in the transfer characteristics was analyzed to investigate the NBIS stability of a-IGZO TFTs with different V_{DS} values using a double-sweeping gate voltage (V_{GS}) mode. The degradation mechanisms resulting from NBIS with different V_{DS} biases were further investigated using capacitance−voltage (C−V) measurements. In the case of NBIS with grounded V_{DS} (V_{GS} = −40 V and V_{DS} = 0 V), the threshold voltage shifted in the negative V_{GS} direction in the forward measurement due to positive charge trapping at the GI/IGZO interface in the initial stage (<1000 s) of the stress. On-current degradation started to be observed in the subsequent stage (>1000 s) of NBIS owing to donor-like defect creation near the conduction band (E_C). These degradations were enhanced by

Received: January 15, 2014
Accepted: April 1, 2014
Published: April 1, 2014

© 2014 American Chemical Society

applying a positive V_{DS} bias of 40 V with NBIS (V_{GS} = −40 V and V_{DS} = 40 V). In contrast, it was found that the NBIS degradations were reduced by applying a small negative V_{DS} bias (V_{GS} = −40 V and V_{DS} = −20 V). Furthermore, the NBIS degradations could be suppressed by applying a large negative V_{DS} bias of $V_{DS} < V_{GS}$ (V_{GS} = −40 V and V_{DS} = −60 V) during NBIS.

2. EXPERIMENTAL PROCEDURE

A schematic cross-sectional view of the bottom-gate IGZO TFT is shown in Figure 1a. The fabrication procedure for the IGZO TFT was

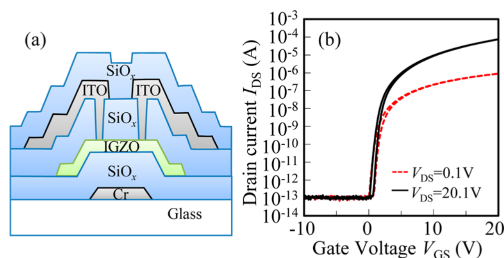

Figure 1. (a) Schematic cross-sectional view and (b) initial transfer curves of bottom-gate IGZO TFT.

as follows. First, a chromium (Cr) gate electrode was formed on a glass substrate. A gate insulator of SiO_x (150 nm) was deposited at 350 °C by plasma-enhanced chemical vapor deposition (PECVD). An IGZO layer with a thickness of 45 nm was then deposited at 160 °C from a sintered IGZO (In:Ga:Zn atomic ratio of 33.8:27.8:38.4) ceramic target by DC magnetron sputtering with a mixed gas of Ar/O_2 = 29.4/0.6 sccm at a deposition pressure of 1 Pa. After patterning of the IGZO as an active channel, a SiO_x film (200 nm) for an etch-stopper was deposited by PECVD. Source and drain electrodes were formed using indium−tin oxide (ITO) via contact holes. A SiO_x passivation layer (200 nm) was further deposited by PECVD. Finally, the IGZO TFTs were annealed in N_2 ambient at 350 °C for 1 h before carrying out the electrical measurements. The channel width (W) to length (L) ratio of the IGZO TFTs was 2.5 (W = 50 μm; L = 20 μm). All current−voltage (I−V) characteristics were measured using an Agilent 4156C precision semiconductor parameter analyzer. The C−V characteristics, the channel capacitance (C_{gc}), the gate-to-source capacitance (C_{gs}), and the gate-to-drain capacitance (C_{gd}) were measured using an Agilent 4980A precision LCR meter at 1 kHz with AC level of 100 mV. All electrical measurements were carried out at room temperature in ambient air.

During the NBIS test, blue light was supplied from a xenon lamp with a band pass filter (460 nm, FWHM of 10 nm) at an intensity of 0.2 mW cm^{-2}. The NBIS was interrupted temporarily when the transfer characteristics were measured by a double-sweeping V_{GS} mode in darkness at V_{DS} of 0.1 V, and then NBIS was reapplied up to an accumulated stress time of 10^4 s. For the double-sweeping V_{GS} mode, transfer characteristics were measured with V_{GS} from −10 to 20 V (denoted hereafter as forward measurement), and then scanned instantly back to −10 V (denoted hereafter as reverse measurement). The V_{GS} stress for all NBIS tests was kept at −40 V, and V_{DS} during NBIS was varied at 40, 0, −20, and −60 V.

3. RESULTS AND DISCUSSION

Figure 1b shows the initial transfer characteristics (I_{DS}−V_{GS}) of a-IGZO TFTs measured at V_{DS} of 0.1 and 20.1 V. A saturation mobility (μ_{sat}) of 13.5 cm^2 V^{-1} s^{-1} was obtained. The SS ($dV_{GS}/d\log_{10}(I_{DS})$) value of 0.60 V/dec. was calculated from V_{GS}, which required I_{DS} from 0.1 to 1 nA. The turn-on voltage of 1.5 V was defined by V_{GS} at I_{DS} of 1 pA. The hysteresis of 0.5 V was defined by the difference of V_{GS} at I_{DS} of 1 nA between the forward and reverse sweeps.

Figure 2a,b shows the variation in the transfer characteristics under NBIS with grounded V_{DS} for the forward and reverse

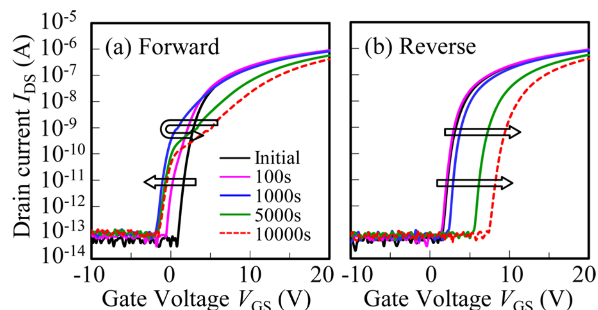

Figure 2. Variation in the transfer characteristics in the (a) forward and (b) reverse measurements as a function of the stress duration for 10^4 s under −40 V V_{GS} NBIS with grounded V_{DS}.

measurements, respectively. For the forward measurements, as shown in Figure 2a, in the initial stage of NBIS (<1000 s), the transfer curves shifted in the negative V_{GS} direction without SS degradation; on-current degradation was then observed in the subsequent stage of NBIS (>1000 s), and this degradation was accelerated with increasing NBIS duration. Note that the negative shift of the transfer curve without SS degradation was observed in the initial stage of NBIS earlier than the on-current degradation phenomenon with SS degradation in the forward measurement. In contrast, for the reverse measurements, as shown in Figure 2b, the transfer curves hardly shifted within the initial NBIS duration of 1000 s, and then these exhibited a parallel shift in the positive V_{GS} direction without SS degradation with increasing NBIS duration. These results indicate that on-current degradation, which was observed in the forward measurements as the NBIS duration exceeded 1000 s, vanished in the reverse measurements. To reveal the degradation mechanism in detail, the variation in the C−V characteristics of the TFT was investigated as the NBIS duration increased, as shown in Figure 3. C−V curves without

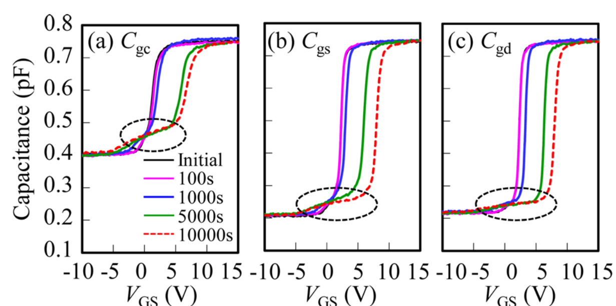

Figure 3. Variation in the C−V curves of (a) C_{gc}, (b) C_{gs}, and (c) C_{gd} as a function of the stress duration for 10^4 s under −40 V V_{GS} NBIS with grounded V_{DS}.

distortion were observed in the initial stage of NBIS (1000 s). When the NBIS duration exceeded 1000 s, the C−V curves shifted in the positive V_{GS} direction with increasing NBIS duration, and distortion of the C−V curves was observed in the off state of the C_{gs}, C_{gd}, and C_{gc} curves, which suggested that the degradation occurred uniformly in the channel under NBIS with grounded V_{DS}.

It has been reported that high-density oxygen vacancies (V_O) exist in the a-IGZO bulk about 2.3 eV away from E_C.[28−30] In

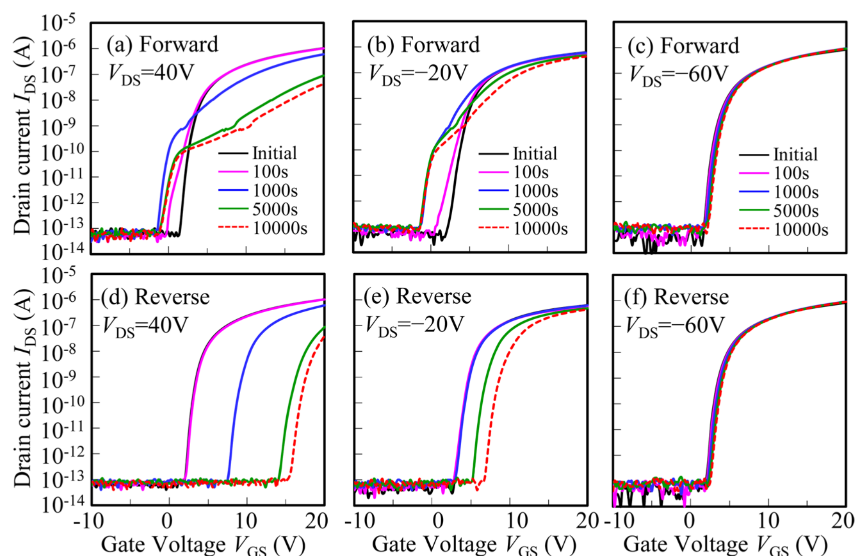

Figure 4. Variation in the transfer characteristics as a function of the stress duration for 10^4 s under −40 V V_{GS} NBIS with V_{DS} biases of (a) 40, (b) −20, and (c) −60 V in the forward measurement, and with V_{DS} biases of (d) 40, (e) −20, and (f) −60 V in the reverse measurement.

this study, the photon energy of the incident light was set to be 2.7 eV, which was sufficient to excite neutral V_O defects to V_O^+ or V_O^{2+}, and to supply free electrons to E_C. Meanwhile, the ionized V_O^+ or V_O^{2+} would be simultaneously neutralized with electrons photoexcitated from the valence band (E_V) to V_O^+ and/or V_O^{2+}, which contributes to free holes in E_V. These photoexcited holes and electrons will be respectively trapped at the GI/IGZO (front-channel) and the IGZO/etch-stopper (back-channel) interfaces under negative V_{GS}. As trapped holes at the front-channel interface have a stronger influence on the transfer curves than trapped electrons at the back-channel interface, hole trapping at the front-channel interface will be the main origin of the negative transfer curve shift without SS degradation in the initial stage (<1000 s) of NBIS in the forward measurement. The trapped holes at the front-channel interface were detrapped immediately on applying the positive V_{GS} during the forward measurement, which resulted in negligible changes in both turn-on voltage and SS in the reverse measurement. This result correlates with the results of the *C*−*V* measurements for NBIS duration of 1000 s.

When the photon energy of the incident light was decreased to less than ∼2.5 eV at an identical intensity of 0.2 mW cm^{-2} (photon flux of 5×10^{18} m^{-2} s^{-1}), negligible changes in both the on-current and SS were observed in the forward measurement and a slightly positive transfer curve shift was observed in the reverse measurement (results not shown here) even for NBIS duration of 10^4 s. This indicated that the NBIS degradations originated from deep subgap states (neutral V_O) existing more than 2.5 eV away from E_C. However, the *C*−*V* results demonstrated that NBIS induced defects in the whole channel near the Fermi level (E_F) at V_{GS} of the turn-on voltage when the NBIS duration exceeded 1000 s. Although the defects originated from V_O^+ and/or V_O^{2+}, the energy levels of V_O^+ and/or V_O^{2+} and the defects showed a large difference. The mechanism for the energy difference between these should be investigated further. Interestingly, the transfer curves exhibited a parallel shift in the positive V_{GS} direction without SS degradation, and the on-current degradation phenomenon in the forward measurement vanished in the subsequent reverse measurement. In our previous study,[31] it was reported that the generated donor-like defects were stabilized by capturing electrons during the forward measurement, and the trapped holes at the front-channel interface were detrapped by the positive V_{GS} during the forward measurement; therefore, electron trapping at the back-channel interface was an origin of the positive shift of the transfer curve without SS degradation in the subsequent reverse measurement.

To investigate the effect of the V_{DS} bias on the NBIS degradation, V_{DS} biases of 40, −20, and −60 V were applied with V_{GS} of −40 V. Figure 4 shows the variation in the transfer characteristics with NBIS duration for each of the V_{DS} values in the forward and reverse measurements. In the case of a positive V_{DS} bias of 40 V with V_{GS} of −40 V, the degradation phenomena were similar to those observed for NBIS with grounded V_{DS}, as shown in Figure 2. However, the on-current exhibited more severe degradation when the NBIS duration was over 1000 s. Following the forward measurement, the positive shift of the transfer curve was significantly greater in the reverse measurement. This result indicates that an additional positive V_{DS} bias of 40 V accelerated donor-like defect creation and electron trapping at the back-channel interface. In contrast to the results obtained from using V_{DS} of 40 V, on-current degradation in the forward measurement and the positive transfer curve shift in the reverse measurement could be reduced by applying a negative V_{DS} of −20 V (V_{GS} = −40 V). When the drain bias (V_{DS}) during NBIS was further decreased to −60 V (V_{GS} = −40 V), it was found that the negative transfer curve shift with on-current degradation, which was observed under NBIS with V_{DS} biases of 40, 0, and −20 V and V_{GS} of −40 V, was suppressed in the forward measurement as shown in Figure 4c. In addition to the forward measurement, the positive shift of the transfer curve, which was observed under NBIS with V_{DS} biases of 40, 0, and −20 V and V_{GS} of −40 V, was also suppressed when V_{DS} = −60 V in the reverse measurement as shown in Figure 4f. These results indicate that the degradations under NBIS can be suppressed by applying a large negative V_{DS} bias ($V_{DS} < V_{GS}$).

To reveal the degradation portion in the active channel, *C*−*V* analyses of C_{gs} and C_{gd} before and after NBIS duration of 10^4 s with different V_{DS} biases were carried out, as shown in Figure 5.

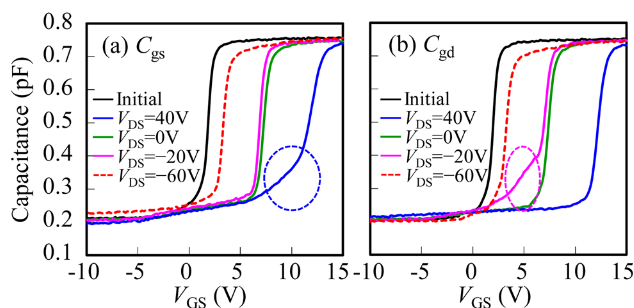

Figure 5. $C-V$ curves of (a) C_{gs} and (b) C_{gd} before and after NBIS duration of 10^4 s with different V_{DS} biases.

On the basis of the $C-V$ results, the energy-band diagrams for the source and drain regions under NBIS with different V_{DS} biases are depicted in Figure 6. The energy band at the drain

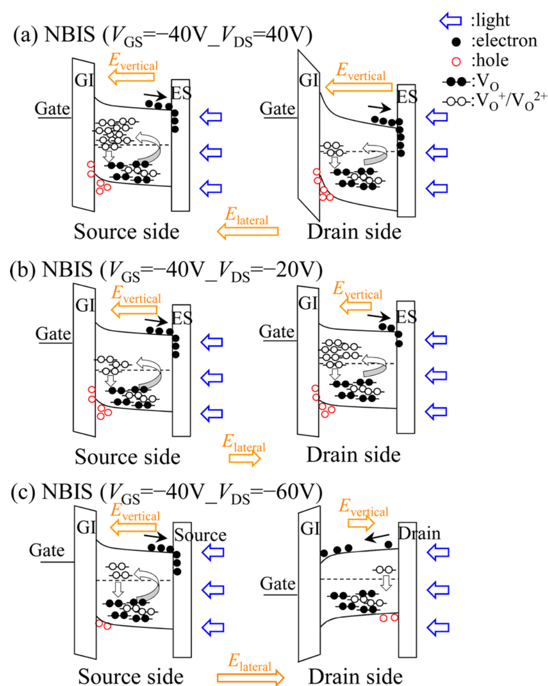

Figure 6. Schematic diagram of degradation mechanism in TFT under NBIS duration of over 1000 s with V_{DS} biases of (a) 40, (b) −20, and (c) −60 V.

side was bent upward more than that at the source side when a V_{DS} bias of 40 V was applied. Comparing the C_{gs} and C_{gd} curves, a hump was only observed at the C_{gs} curve near the turn-on region at a V_{DS} bias of 40 V, indicating that the energy level of the generated defects was near E_F at V_{GS} of turn-on voltage near the source side. Thus, NBIS with an additional positive V_{DS} bias of 40 V accelerated donor-like defect creation near the source side, leading to degradation of the drain current above the turn-on region. Both the C_{gs} and C_{gd} curves shifted in the more positive V_{GS} direction than those at V_{DS} = 0 V, indicating that more electrons were trapped at the back-channel interface due to an increase in the vertical electric fields in the channel.

When the V_{DS} bias changed from 40 to −20 V, it was noted that a distinct hump was observed near the turn-on region of the C_{gd} curve rather than of the C_{gs} curve. The fact that the appearance of the hump changed from the C_{gs} to the C_{gd} curve indicated that the defect generation changed from the source to the drain side, when the V_{DS} bias varied from 40 to −20 V. This result indicates that, although positively charged V_O^+ and/or V_O^{2+} were generated in the whole channel due to the photoexcitation irrespective of V_{DS} bias, these positive charges drifted and accumulated as a result of the lateral electric field induced by the V_{DS} bias. The smaller positive shift of both C_{gs} and C_{gd} curves at V_{DS} of −20 V than that at V_{DS} = 0 V indicated that fewer electrons were trapped at the back-channel interface due to a decrease of the vertical electric field in the channel. As a consequence, drain current degradation above the turn-on region in the forward measurement and the positive transfer curve shift in the reverse measurement were reduced when a negative V_{DS} bias of $V_{DS} > V_{GS}$ was applied.

When the V_{DS} bias was further decreased to −60 V ($V_{DS} < V_{GS}$), it should be noted that both the C_{gs} and C_{gd} curves after NBIS (with V_{GS} bias of −40 V) slightly shifted as compared with grounded V_{DS}. Figure 6c shows the gate-to-source and gate-to-drain energy-band diagrams during NBIS with V_{DS} bias of −60 V. In this case, although positively charged V_O^+ and/or V_O^{2+} will be accumulated near the drain side as a result of the lateral electric field, no defect generation was observed in the C_{gd} curve. This result indicates that the electron concentration in the channel had a strong impact on the generation of donor-like states because the drain side of the channel changed from depletion to accumulation condition when the V_{DS} bias varied from −20 to −60 V. The accumulated V_O^+ or V_O^{2+} near the drain region will be easily recombined and stabilized with electrons injected from the drain electrode;[31] therefore, donor-like defect creation can be suppressed by applying a large negative V_{DS} bias of $V_{DS} < V_{GS}$. In addition, the free holes generated under NBIS are accumulated and are drained to the drain electrode because it has the lowest potential for positive charges. Because of a few holes being trapped at the front-channel interface, the negative shift of the transfer curve can be suppressed in the forward measurement. Moreover, electron trapping at the back-channel interface will also be reduced by applying a large negative V_{DS} bias of $V_{DS} < V_{GS}$, leading to the decrease in the positive transfer curve and shifts in $C-V$ curve.

On the basis of the $C-V$ analysis with different V_{DS} biases, it was clarified that the photoexcited positively charged V_O^+ or V_O^{2+} were caused to drift by the lateral electric field, and these were the main origin of donor-like defect creation during NBIS. A large negative V_{DS} bias of $V_{DS} < V_{GS}$ changed the drain region to the accumulation condition; therefore, the NBIS degradation can be suppressed by the neutralization of accumulated positively charged V_O^+ or V_O^{2+} with electrons in the drain region.

4. CONCLUSION

In this study, the effect of the V_{DS} bias on the NBIS stability of a-IGZO TFTs was investigated. The degradation mechanisms of a-IGZO TFTs under NBIS with different V_{DS} biases were revealed using $I-V$ and $C-V$ characteristics. In the initial stage of NBIS with grounded V_{DS} (V_{GS} = −40 V and V_{DS} = 0 V), the transfer curves shifted negatively with insignificant SS degradation because of hole trapping at the front-channel interface under NBIS. On the other hand, on-current degradation occurred, which was accelerated as the NBIS duration increased in the forward measurement; the degradations originated from the creation of donor-like defects near E_C. However, the donor-like defects could be stabilized by capturing electrons in the forward measurement, resulting in

dx.doi.org/10.1021/am500300g | ACS Appl. Mater. Interfaces 2014, 6, 5713−5718

the transfer curve shifting parallel in the positive V_{GS} direction without on-current degradation in the reverse measurement. NBIS with an additional positive V_{DS} bias (V_{GS} = −40 V and V_{DS} = 40 V) accelerated the donor-like state creation near the source side because of the positively charged V_O^+ and/or V_O^{2+} drifting from the drain to the source side under the influence of the lateral electric field, which contributed to more severe on-current degradation. In contrast to the results obtained using V_{DS} of 40 V, on-current degradation in the forward measurement and the positive transfer curve shift in the reverse measurement can be reduced, due to fewer electrons being trapped at the back-channel interface under the weak vertical electric field, by applying a small negative V_{DS} bias of $V_{DS} > V_{GS}$ (V_{GS} = −40 V and V_{DS} = −20 V) during NBIS. Furthermore, the NBIS degradation was significantly suppressed by applying a large negative V_{DS} bias of $V_{DS} < V_{GS}$ (V_{GS} = −40 V and V_{DS} = −60 V), because the positive charges of V_O^+ and V_O^{2+} were easily neutralized by electrons under the accumulation condition in the drain region. This study clarified that the photoexcited positively charged V_O^+ and/or V_O^{2+} were the main origin of donor-like defect creation during NBIS, and the positive charges were caused to drift by the lateral electric field. We consider that a promising method to suppress NBIS degradation is to apply a large negative V_{DS} bias of $V_{DS} < V_{GS}$ during NBIS.

■ AUTHOR INFORMATION

Corresponding Authors

*E-mail: wang.dapeng@kochi-tech.ac.jp.
*E-mail: furuta.mamoru@kochi-tech.ac.jp.

Notes

The authors declare no competing financial interest.

■ ACKNOWLEDGMENTS

Part of this work was supported by a grant from the Japan Society for the Promotion of Science, Grant-in-Aid for Scientific Research (C), No. 23560408. The authors would like to thank Idemitsu Kosan Co. Ltd., for their support throughout this work.

■ REFERENCES

(1) Hirao, T.; Furuta, M.; Hiramatsu, T.; Matsuda, T.; Li, C.; Furuta, H.; Hokari, H.; Yoshida, M.; Ishii, H.; Kakegawa, M. Bottom-Gate Zinc Oxide Thin-Film Transistors (ZnO TFTs) for AM-LCDs. *IEEE Trans. Electron Devices* **2008**, *55*, 3136−3142.

(2) Nomura, K.; Ohta, H.; Takagi, A.; Kamiya, T.; Hirano, M.; Hosono, H. Room-Temperature Fabrication of Transparent Flexible Thin-Film Transistors Using Amorphous Oxide Semiconductors. *Nature* **2004**, *432*, 488−492.

(3) Takechi, K.; Nakata, M.; Eguchi, T.; Yamaguchi, H.; Kaneko, S. Temperature-Dependent Transfer Characteristics of Amorphous $InGaZnO_4$ Thin-Film Transistors. *Jpn. J. Appl. Phys.* **2009**, *48*, 011301-1−011301-6.

(4) Nomura, K.; Takagi, A.; Kamiya, T.; Ohta, H.; Hirono, M.; Hosono, H. Amorphous Oxide Semiconductors for High-Performance Flexible Thin-Film Transistors. *Jpn. J. Appl. Phys.* **2006**, *45*, 4303−4308.

(5) Hwang, T.-H.; Yang, I.-S.; Kwon, O.-K.; Ryu, M.-K.; Byun, C.-W.; Hwang, C.-S.; Park, S.-H. K. Inverters Using Only N-Type Indium Gallium Zinc Oxide Thin Film Transistors for Flat Panel Display Applications. *Jpn. J. Appl. Phys.* **2011**, *50*, 03CB06-1−03CB06-4.

(6) Ohara, H.; Sasaki, T.; Noda, K.; Ito, S.; Sasaki, M.; Endo, Y.; Yoshitomi, S.; Sakata, J.; Serikawa, T.; Yamazaki, S. 4.0-Inch Active-Matrix Organic Light-Emitting Diode Display Integrated with Driver Circuits Using Amorphous In−Ga−Zn-oxide Thin-Film Transistors with Suppressed Variation. *Jpn. J. Appl. Phys.* **2010**, *49*, 03CD02-1−03CD02-6.

(7) Godo, H.; Kawae, D.; Yoshitomi, S.; Sasaki, T.; Ito, S.; Ohara, H.; Kishida, H.; Takahashi, M.; Miyanaga, A.; Yamazaki, S. Temperature Dependence of Transistor Characteristics and Electronic Structure for Amorphous In−Ga−Zn−Oxide Thin Film Transistor. *Jpn. J. Appl. Phys.* **2010**, *49*, 03CB04-1−03CB04-6.

(8) Tsai, C.-T.; Chang, T.-C.; Chen, S.-C.; Lo, I.; Tsao, S.-W.; Hung, M.-C.; Chang, J.-J.; Wu, C.-Y.; Huang, C.-Y. Influence of Positive Bias Stress on N_2O Plasma Improved InGaZnO Thin Film Transistor. *Appl. Phys. Lett.* **2010**, *96*, 242105-1−242105-3.

(9) Kim, M.; Jeong, J. H.; Lee, H. J.; Ahn, T. K.; Shin, H. S.; Park, J.-S.; Jeong, J. K.; Mo, Y.-G.; Kim, H. D. High Mobility Bottom Gate InGaZnO Thin Film Transistors with SiO_x Etch Stopper. *Appl. Phys. Lett.* **2007**, *90*, 212114-1−212114-3.

(10) Yabuta, H.; Sano, M.; Abe, K.; Aiba, T.; Den, T.; Kumomi, H.; Nomura, K.; Kamiya, T.; Hosono, H. High-Mobility Thin-Film Transistor with Amorphous $InGaZnO_4$ Channel Fabricated by Room Temperature RF-Magnetron Sputtering. *Appl. Phys. Lett.* **2006**, *89*, 112123-1−112123-3.

(11) Takechi, K.; Nakata, M.; Azuma, K.; Yamaguchi, H.; Kaneko, S. Dual-Gate Characteristics of Amorphous $InGaZnO_4$ Thin-Film Transistors as Compared to Those of Hydrogenated Amorphous Silicon Thin-Film Transistors. *IEEE Trans. Electron Devices* **2009**, *56*, 2027−2033.

(12) Chen, C.; Abe, K.; Fung, T. C.; Kumomi, H.; Kanicki, J. Amorphous In−Ga−Zn−O Thin Film Transistor Current-Scaling Pixel Electrode Circuit for Active-Matrix Organic Light-Emitting Displays. *Jpn. J. Appl. Phys.* **2009**, *48*, 03B025-1−03B025-7.

(13) Kwon, J. Y.; Son, K. S.; Jung, J. S.; Kim, T. S.; Ryu, M. K.; Park, K. B.; Yoo, B. W.; Kim, J. W.; Lee, Y. G.; Park, K. C.; Lee, S. Y.; Kim, J. M. Bottom-Gate Gallium Indium Zinc Oxide Thin-Film Transistor Array for High-Resolution AMOLED Display. *IEEE Electron Device Lett.* **2008**, *29*, 1309−1311.

(14) Lee, K.-H.; Jung, J. S.; Son, K. S.; Park, J. S.; Kim, T. S.; Choi, R.; Jeong, J. K.; Kwon, J.-Y.; Koo, B.; Lee, S. The Effect of Moisture on the Photon-Enhanced Negative Bias Thermal Instability in Ga−In−Zn−O Thin Film Transistors. *Appl. Phys. Lett.* **2009**, *95*, 232106-1−232106-3.

(15) Chang, Y.-G.; Moon, T.-W.; Kim, D.-H.; Lee, H. S.; Kim, J. H.; Park, K.-S.; Kim, C.-D.; Im, S. DC Versus Pulse-Type Negative Bias Stress Effects on the Instability of Amorphous InGaZnO Transistors Under Light Illumination. *IEEE Electron Device Lett.* **2011**, *32*, 1704−1706.

(16) Ji, K. H.; Kim, J.-I.; Mo, Y.-G.; Jeong, J. H.; Yang, S.; Hwang, C.-S.; Park, S.-H. K.; Ryu, M.-K.; Lee, S.-Y.; Jeong, J. K. Comparative Study on Light-Induced Bias Stress Instability of IGZO Transistors With SiN_x and SiO_2 Gate Dielectrics. *IEEE Electron Device Lett.* **2010**, *31*, 1404−1406.

(17) Oh, H.; Yoon, S.-M.; Ryu, M. K.; Hwang, C.-S.; Yang, S.; Park, S.-H. K. Transition of Dominant Instability Mechanism Depending on Negative Gate Bias under Illumination in Amorphous In−Ga−Zn−O Thin Film Transistor. *Appl. Phys. Lett.* **2011**, *98*, 033504-1−033504-3.

(18) Nomura, K.; Kamiya, T.; Hirano, M.; Hosono, H. Origins of Threshold Voltage Shifts in Room-Temperature Deposited and Annealed a-In−Ga−Zn−O Thin-Film Transistors. *Appl. Phys. Lett.* **2009**, *95*, 013502-1−013502-3.

(19) Kim, B.; Chong, E.; Kim, D. H.; Jeon, Y. W.; Kim, D. H.; Lee, S. Y. Origin of Threshold Voltage Shift by Interfacial Trap Density in Amorphous InGaZnO Thin Film Transistor under Temperature Induced Stress. *Appl. Phys. Lett.* **2011**, *99*, 062108-1−062108-3.

(20) Chen, T. C.; Chang, T. C.; Hsieh, T. Y.; Tsai, C. T.; Chen, S. C.; Lin, C. S.; Jian, F. Y.; Tsai, M. Y. Investigation of the Gate-Bias Induced Instability for InGaZnO TFTs under Dark and Light Illumination. *Thin Solid Films* **2011**, *520*, 1422−1426.

(21) Suresh, A.; Muth, J. F. Bias Stress Stability of Indium Gallium Zinc Oxide Channel Based Transparent Thin Film Transistors. *Appl. Phys. Lett.* **2008**, *92*, 033502-1−033502-3.

(22) Oh, H.; Yoon, S.-M.; Ryu, M. K.; Hwang, C.-S.; Yang, S.; Park, S.-H. K. Photon-Accelerated Negative Bias Instability Involving Subgap States Creation in Amorphous In−Ga−Zn−O Thin Film Transistor. *Appl. Phys. Lett.* **2010**, *97*, 183502-1−183502-3.

(23) Shimakawa, S.; Wang, D.; Furuta, M. Photo Induced Negative Bias Instability of Zinc Oxide Thin-Film Transistors. *Jpn. J. Appl. Phys.* **2012**, *51*, 108003-1−108003-2.

(24) Huang, S.-Y.; Chang, T.-C.; Lin, L.-W.; Yang, M.-C.; Chen, M.-C.; Jhu, J.-C.; Jian, F.-Y. The Asymmetrical Degradation Behavior on Drain Bias Stress under Illumination for InGaZnO Thin Film Transistors. *Appl. Phys. Lett.* **2012**, *100*, 222901-1−222901-3.

(25) Um, J.-G.; Mativenga, M.; Migliorato, P.; Jang, J. Increase of Interface and Bulk Density of States in Amorphous-Indium−Gallium−Zinc−Oxide Thin-Film Transistors with Negative-Bias-under-Illumination-Stress Time. *Appl. Phys. Lett.* **2012**, *101*, 113504-1−113504-3.

(26) Fujii, M.; Yano, H.; Hatayama, T.; Uraoka, Y.; Fuyuki, T.; Jung, J. S.; Kwon, J. Y. Thermal Analysis of Degradation in Ga_2O_3−In_2O_3−ZnO Thin-Film Transistors. *Jpn. J. Appl. Phys.* **2008**, *47*, 6236−6240.

(27) Hsieh, T.-Y.; Chang, T.-C.; Chen, T.-C.; Tsai, M.-Y.; Chen, Y.-T.; Jian, F.-Y.; Chung, Y.-C.; Ting, H.-C.; Chen, C.-Y. Investigating the Drain-Bias-Induced Degradation Behavior under Light Illumination for InGaZnO Thin-Film Transistors. *IEEE Electron Device Lett.* **2012**, *33*, 1000−1002.

(28) Nomura, K.; Kamiya, T.; Hosono, H. Highly Stable Amorphous In−Ga−Zn−O Thin-Film Transistors Produced by Eliminating Deep Subgap Defects. *Appl. Phys. Lett.* **2011**, *99*, 053505-1−053505-3.

(29) Nomura, K.; Kamiya, T.; Yanagi, H.; Ikenaga, E.; Yang, K.; Kobayashi, K.; Hirano, M.; Hosono, H. Subgap States in Transparent Amorphous Oxide Semiconductor, In−Ga−Zn−O, Observed by Bulk Sensitive X-Ray Photoelectron Spectroscopy. *Appl. Phys. Lett.* **2008**, *92*, 202117-1−202117-3.

(30) Lee, K.; Nomura, K.; Yanagi, H.; Kamiya, T.; Hosono, H. Photovoltaic Properties of N-Type Amorphous In−Ga−Zn−O and P-Type Single Crystal Si Heterojunction Solar Cells: Effects of Ga Content. *Thin Solid Films* **2012**, *520*, 3808−3812.

(31) Hung, M. P.; Wang, D.; Jiang, J.; Furuta, M. Negative Bias and Illumination Stress Induced Electron Trapping at Back-Channel Interface of InGaZnO Thin Film Transistor. *ECS Solid State Letters* **2014**, *3* (3), Q13−Q16.